

Junction Characteristics and Magnetic Field Dependencies of Low Noise Step Edge Junction Rf-SQUIDs for Unshielded Applications

Mehdi Fardmanesh, *Senior Member, IEEE*, Juergen Schubert, Rizwan Akram, Ali Bozbey, Marcel Bick, Marko Banzet, D. Lomparski, Willi Zander, Yi Zhang, and Hans-Jochen Krause

Abstract—Step edge grain boundary (GB) junctions and rf-SQUIDs have been made using pulsed laser deposited Y-Ba-Cu-O films on crystalline LaAlO₃ substrates. The steps were developed using various ion-beam etching processes resulting in sharp and ramp type step structures. Sharp step based GB junctions showed behavior of serial junctions with resistively shunted junction (RSJ)-like I - V characteristics. The ramped type step structures resulted in relatively high critical current, I_c , junctions and noisy SQUIDs. The sharp steps resulted in low noise rf-SQUIDs with a noise level below $140 \text{ fT}/\text{Hz}^{1/2}$ down to few Hz at 77 K while measured with conventional tank circuits. The I_c of the junctions and hence the operating temperature range of the SQUIDs made using sharp steps was controlled by both the step height and the junction widths. The junction properties of the SQUIDs were also characterized showing RSJ-like characteristics and magnetic field sensitivities correlated to that of the SQUIDs. Two major low and high background magnetic field sensitivities have been observed for our step edge junctions and the SQUIDs made on sharp steps. High quality step edge junctions with low magnetic field sensitivities made on clean sharp steps resulted in low $1/f$ noise rf-SQUIDs proper for applications in unshielded environment.

Index Terms—Grain boundary, Josephson junction, magnetic field, noise, rf-SQUID.

I. INTRODUCTION

ONE of the very early applications of the step edge junction (SEJ) has been in the fabrication of rf-SQUIDs [1], where e.g., the bi-crystal grain boundary (GB) partly limits the layout designs due to the extension of the GB across the substrates [2]–[5]. Step edge GB Josephson junctions (JJs) provide high flexibility in the layout designs due to flexibility in their positions on the chips. Though, the difficulties in the control of the parameters of the SEJs have been a drawback in this technology [1]. This is partly due to the difficulties in control of the step structure made onto the substrates, and the growth of high quality film at the steps [1], [6]. The extensive works on SEJ technology has resulted in low $1/f$ -type and white noise

rf-SQUIDs with flexible optimal layout design and chip integration [1], [6]–[8]. We have obtained low $1/f$ noise and magnetically stable SEJ rf-SQUIDs on crystalline LaAlO₃ substrates through the control of the step structure leading to growth of high quality Y-Ba-Cu-O film at the junctions. We have observed two major low and high magnetic field dependencies in our SEJs and the resulting SEJ rf-SQUIDs. At the same time we have also observed various nonclassical magnetic field dependencies as previously reported [9], [10]. The applied magnetic field (B_A) dependence of the flux-voltage transfer function signal, V_{s-pp} , of the SQUIDs was correlated to the characteristics of their SEJs for both types of the field dependencies. The characteristics of the JJs of the SQUIDs could be investigated by opening the flux focusing washer areas of the devices. In this work we report on the structural dependence, electrical characteristics, and magnetic field dependencies of our SEJs and the characteristics of the resulting rf-SQUIDs made using the SEJ technology.

II. SAMPLE PREPARATION AND CHARACTERISATION SETUP

Sharp and ramp type step structures were made onto LaAlO₃ (100) substrates using various stationary and angled argon ion beam etching (IBE) processes. The steps were made by making up to $10 \mu\text{m}$ wide ditches onto the substrates. Sharp clean steps with angles close to 90° and flat substrate surfaces at the steps were obtained using an optimized “Combinational IBE” (CIBE) process, the high resolution SEMs of which are reported elsewhere [11]. This was made using a relatively low intensity ($\sim 0.1 \text{ mA}/\text{cm}^2$) and high energy (500–600 eV) stationary 40° angled ion beam along the step edges to reach the approximate desired step height, and using a lower energy ($\sim 300 \text{ eV}$) rotating 45° angled ion beam to get surface modified steps. Ramp-type steps were made using stationary 40° – 45° angled ion beams perpendicular to the edges of the ditches in the substrates. The ditches were patterned onto the substrates, using modified photolithography process to obtain sharp photo-resist shadow mask patterns. A 60 nm thick e-beam evaporated gold layer was deposited onto the substrates prior to the IBE to obtain clean step edges. High quality films with smooth morphology at the steps could be obtained on LaAlO₃ substrates, with steps prepared using the above CIBE process. The films were deposited by pulsed laser deposition technique using a KrF Excimer laser and patterned using conventional photolithography and IBE techniques [11]. The SQUIDs were made with our typical rf-SQUID magnetometer layout design carrying $100 \mu\text{m}$ by $100 \mu\text{m}$ loop

Manuscript received August 5, 2002. This work was supported by research and development project number 42.6.I3 B.2.A.

M. Fardmanesh, R. Akram, and A. Bozbey are with the Electrical and Electronics Engineering Department, Bilkent University, 06533 Ankara, Turkey and also with ISG-2, Research Center Juelich (FZJ), 52425 Juelich, Germany (e-mail: m.fardmanesh@fz-juelich.de).

J. Schubert, M. Banzet, D. Lomparski, W. Zander, Y. Zhang, and H.-J. Krause are with FZJ, 52425 Juelich, Germany.

M. Bick is with CSIRO Telecommunication and Industrial Physics, Lindfield, NSW 2070, Australia.

Digital Object Identifier 10.1109/TASC.2003.814060

and 3.6 mm diameter washer area [6], [7]. A Helium dewar based characterization setup with a two layer μ -metal magnetic shield and a temperature stability of better than 0.1 K was used to characterize the samples.

III. SEJ I - V CHARACTERISTICS AND MAGNETIC FIELD DEPENDENCE

SEJs were made on various step structures. The I_c of the junctions was highly sensitive to the uniformity of the films and microstructure of the steps, investigated by high resolution SEM [6], [11]. The average I_c of our SEJs decreased as the step heights increased from about 150 nm to about 270 nm. The SEJs made on our 150 nm deep ditches resulted in about one order of magnitude higher I_c values compared to that of the 200–270 nm deep ditches with mostly flux flow characteristics. Quality SEJs made on sharp steps with step heights above 200 nm, showed mostly RSJ-like characteristics. While the I_c of arrays of test junctions increased as the junction width (W) increased, a systematic dependence of the I_c on the W was not obtained. Our ramp-type step structures typically resulted in very high I_c values compared to the sharp steps. SQUIDS made of ramp type steps showed very high operating temperature ranges close to the T_c of the films with high $1/f$ -type noise spectra [6], [11], [12]. The SEJs and SEJ rf-SQUIDS studied in the following were made on sharp clean CIBE step structures. Four serial junctions can be principally obtained in this configuration when a superconducting film bridges a ditch with sharp trenches, resulting in two junctions at each step [1], [6], [11]. I - V curves and the corresponding dV/dI curves of a 2 μm wide junction of a low noise rf-SQUID on 270 nm deep ditch are shown in Fig. 1(a) and (b), respectively. While the I - V curves in Fig. 1 show an RSJ-like behavior, some of the junctions showed mixed behavior of RSJ and non-RSJ type characteristics.

As shown in Fig. 1(b), relatively high R_N values were obtained for our samples. The R_N of our SEJs was in the range of a few 10 s of Ohms for junction widths in the range of a few micrometers. The R_N values of the RSJ-like behavior junctions were also decreased with increase of the temperature as shown in Fig. 1. Scaling of R_N and I_c of the junctions with the geometrical junction widths, resulted in close $I_c R_N$ products in the range of 1 mV at $T < 10$ K for various junction widths.

The I - V curve of a 3 μm wide junction with low hysteretic behavior ($I_{c-\text{min}}/I_{c-\text{max}} = 0.95$ at $B_A = 0$) is shown in Fig. 2. The I - V curves were obtained by ramping the current from negative value to the maximum positive values as shown by arrows in Fig. 2. The associated Stewart McCumber parameter, $\beta_c = 4\pi e I_c C R^2 / h$ [13], resulted in a junction capacitance of about 2 fF, below the expected typical reported values for Y-Ba-Cu-O GB JJs [14]–[16]. The relatively low capacitance and high R_N values of our SEJs suggest effective junction areas much smaller than the “geometrical area” of the junctions [6], [9]. The hysteretic I - V characteristics could not be observed for our SEJs with low I_c . This was mainly associated to the low ratio of Josephson coupling coefficient to the thermal fluctuations or simply high junction noise parameters, $\Gamma = 2\pi K_B T / I_c \phi_0$ [9].

As shown in Fig. 2, I - V curves of the junctions showed slight nonlinear behavior at $V \approx I_c R_N$ with deviation from the simple

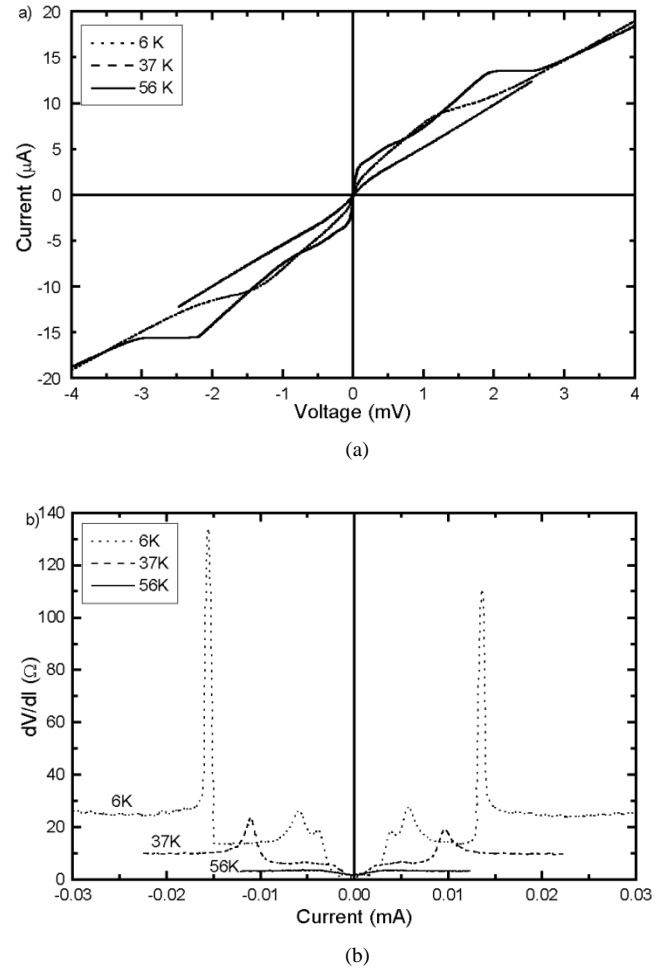


Fig. 1. Temperature dependence of, (a) I - V curve and (b) dV/dI versus I of the junction of an rf-SQUID magnetometer made on LaAlO_3 substrate with 260 nm deep CIBE steps.

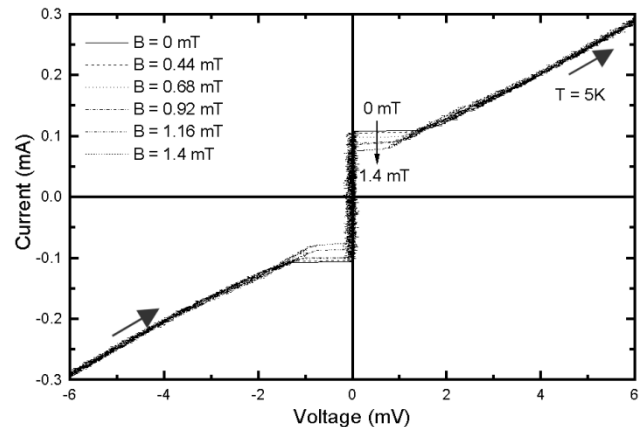


Fig. 2. Magnetic field dependence of the I - V curves of a low field-sensitive 3 μm wide junction made on 260 nm deep CIBE steps.

RSJ-model at low temperatures. This is similar to that associated with the Josephson flux motion effect happening in junctions with widths of about 4 times larger than the Josephson penetration depth, $\lambda_j = (h/4\pi e J_c \mu_0 (2\lambda + d))^{0.5}$ [13]. The W/λ_j values for our SEJs were obtained using the geometrical widths

of the junction. The obtained W/λ_J ratios were about the reported values for these types of the junctions and our bicrystal GB junctions with similar junction widths [5], [14], [16]. The junction of Fig. 2 showed clear linear RSJ type I - V characteristics at temperatures higher than about 15 K, corresponding to approximate $W/\lambda_J < \sim 2$ as also obtained for our bicrystal GB JJs [5]. The dV/dI versus temperature of the samples was used to determine the clear RSJ-like behavior. The above suggests effective junction area proportional to “ W ” as also confirmed by the dependence of the I_c on the junction widths.

Mixed low and high B_a dependencies of the I_c was observed for our SEJs made on sharp CIBE steps. Our SEJs with high field-sensitivities showed B_a dependencies scaling with the $1/W^2$ ratio [9], [17]. I_c of the step edge junction with low field-sensitivities showed very low B_a dependencies up to 1.4 mT, the limit of our characterization setup. Magnetic field dependence of the low field-sensitive SEJs could not be correlated to the I_c or the geometrical width of the junctions. This might be associated to be due to the physical position of the low I_c junctions at the steps and their orientation with respect to the B_a . The mixed B_a dependencies of the junctions resulted in two distinct magnetic field behavior of the SQUIDS discussed in the followings.

IV. SEJ RF-SQUID CHARACTERISTICS AND MAGNETIC FIELD DEPENDENCIES

Low $1/f$ noise rf-SQUIDS were obtained using quality films on sharp steps on LaAlO_3 . The step structure dependencies of the operating temperature range (ΔT_{op}), background magnetic field sensitivity (B_B), and noise characteristics of the SQUIDS were investigated. The characteristics of the junctions of the SQUIDS were also investigated by opening the washer areas of the devices.

A. ΔT_{op} and SQUID Junction Characteristics

The dependence of the ΔT_{op} of the SQUIDS on the CIBE step structures was investigated by measuring the $V_{s\text{-pp}}$ signal of the devices versus the step height and the SQUID junction widths. Low step heights resulted in high ΔT_{op} ranges. This was in agreement with the I_c measurement of the junctions of the SQUIDS as well as the test junction-arrays on similar type of the steps. This was done by investigating the optimal rf-SQUID parameter, $\beta_L = 2\pi LI_c/\Phi_0 \cong 1$, for the used layouts [7], [9]. Decrease of the junction width for the same step heights reduced the ΔT_{op} of the devices, a detailed study of which is previously reported [6], [11]. While the white noise level in our devices could mostly be correlated to their $V_{s\text{-pp}}$, the $1/f$ -type noise spectra was observed to be mostly dependent on the quality of the steps and the films at the steps, inspected by high resolution SEM [6], [12]. The noise spectrum of a low B_B sensitive sample, measured in liquid nitrogen (for temperature stability) using an optimal conventional L-C tank circuit, is shown in Fig. 3. Detailed study of dependence of the $V_{s\text{-pp}}$ of our rf-SQUIDS with various junction widths on LaAlO_3 with various CIBE step structures is presented elsewhere [6], [11].

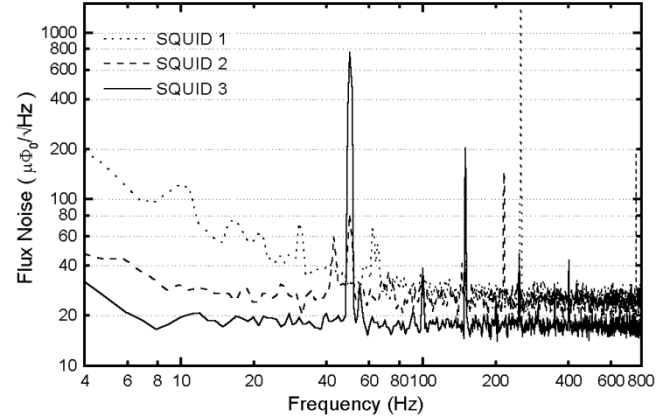


Fig. 3. Noise spectra of rf-SQUIDS with high field-sensitivity (SQUID 1) and low field-sensitivity (SQUIDS 2 and 3) characteristics. SQUID 3 is measured in liquid nitrogen using optimal L-C tank circuit.

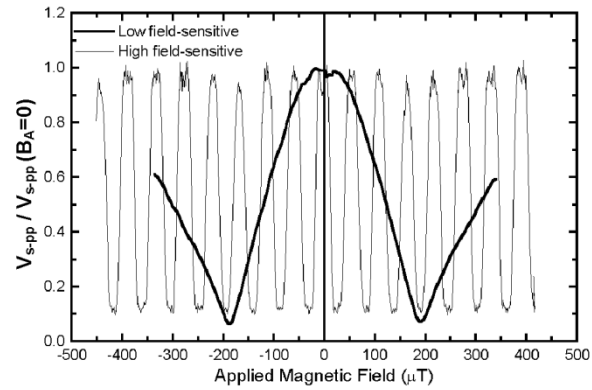


Fig. 4. Normalized magnetic field dependence of flux voltage transfer function signal for low field-sensitive and high field-sensitive rf-SQUIDS with zero field $V_{s\text{-pp}}$ of 0.6 V and 0.5 V, respectively.

B. Magnetic Field Dependence

Two distinct applied background magnetic field, B_B , sensitivities were observed for our rf-SQUIDS made on sharp CIBE steps. While some SQUIDS showed high B_B sensitivities, others showed much lower B_B sensitivities resulting in relatively magnetically stable devices under earth magnetic field. Both type of the test devices had a geometrical junction width of 2–3 μm patterned using IBE process. The field dependencies of $V_{s\text{-pp}}$ of two rf-SQUIDS with high and low B_B sensitivities are shown in Fig. 4. The magnetic field dependence of the I_c of the SQUID junctions of Fig. 4 was measured after opening the flux focusing washer area of the devices. The I_c s were measured using a voltage criterion across the junctions under ramping bias current at various B_A values. The B_A dependence of the I_c of the junction in Fig. 5, followed that of the $V_{s\text{-pp}}$ of the high field-sensitive SQUID shown in Fig. 4 with a slight discrepancy associated to calibration accuracy of the fields. Similar behavior of such B_B sensitivity of our rf-SQUIDS and its correlation with the parameters of the junctions of the devices is previously reported [9]. The study of the drop of the $V_{s\text{-pp}}$ of high B_B sensitive devices led to the need of rf-SQUID layout designs with junction widths in the

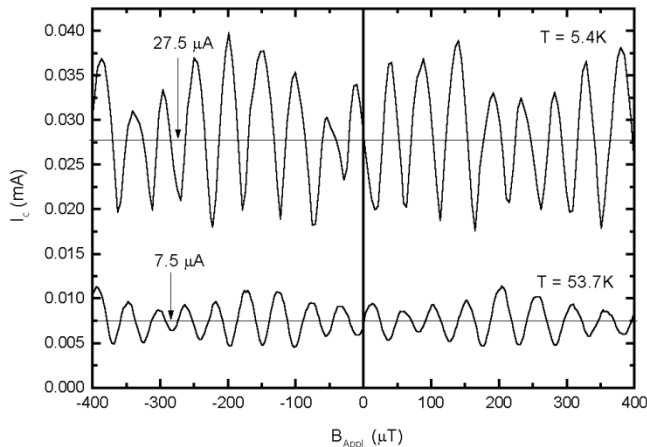


Fig. 5. Magnetic field dependence of I_c of the junction of high field-sensitive rf-SQUID in Fig. 4 at low and high temperatures.

range of 0.6–1.2 μm to obtain magnetically stable devices for applications in unshielded environment [9].

We also obtained low noise magnetically stable rf-SQUIDS with 2–3 μm wide junctions, proper for operation under earth magnetic field [9]. The V_{s-pp} signal of the magnetically stable devices dropped by less than about 10% under $B_A \sim 50 \mu\text{T}$. The field dependence of the I_c of the junctions of SQUID with similar low B_B sensitivities shown in Fig. 4, also showed low field dependencies in agreement with the field dependencies of the corresponding SQUIDS. This was also consistent with the field dependence for some isolated test junctions, showing very low B_A dependence as shown in Fig. 2. The field sensitivity of the test junctions was correlated to that of the SQUID junctions through the effective area of their patterns [9]. Effect of the flux focusing area of the SQUIDS, allowed the observation of the B_A dependence of the SQUID junctions below $B_A = 1 \text{ mT}$ by intensifying the field at the junction.

The low and high B_B sensitivities of the SQUIDS might be associated to the physical position of the working junction of the devices at the steps and their orientation with respect to the B_A , as junctions with shielded effective area or an area parallel to the B_A are expected to have low field sensitivity. Typical noise spectra of low noise devices having various magnetic field sensitivities measured at their optimal operating temperatures are shown in Fig. 3. The studied devices in this work with lower B_B sensitivities showed lower $1/f$ noise levels compared to that of the higher B_B sensitive devices. The work for correlating the noise characteristics and B_B dependence of the SQUIDS to the characteristic parameters and structure of their junctions is further in progress. This is to obtain higher yield of low noise devices with magnetically stable characteristics for applications such as NDE, MCG, and SQUID microscopy in unshielded environment.

V. SUMMARY AND CONCLUSIONS

Sharp clean steps with flat substrate surfaces at the steps made using an optimized combinational IBE process, favorably resulted in low J_c SEJs. The I_c of our SEJs decreased as the step height increased and showed an approximate junction effective

area proportional to the geometric width of the junction. SEJs made of quality films on sharp steps showed RSJ-like behavior with hysteretic nonlinear I - V characteristics at low temperatures leading in capacitances in the range of 0.5–2.5 $\mu\text{F}/\text{cm}^2$.

Two major field dependencies were observed for our devices under the applied magnetic field. A relatively high field sensitivity of the I_c for some of our test junctions and the rf-SQUID junctions was observed which has previously been reported and associated to the junction widths. This kind of SEJs resulted in SQUIDS with high B_B sensitivities improper for operation under unshielded environment. A relatively low field sensitivity for I_c of other test junctions and the SQUID junctions has been observed which has resulted in SQUIDS with low B_B sensitivities proper for operation under the earth magnetic field. All the test devices had junction widths 2–3 μm . The low B_B sensitivity of our junctions and the resulting magnetically stable SQUIDS might be associated to the physical position of the determining GB JJs at the steps and its relative orientation with respect to the applied field. Magnetically stable, low $1/f$ noise devices have been obtained by high quality defect free films developed on sharp steps with flat surfaces at the step edges made using optimized low intensity IBE process, proper for NDE, MCG, and SQUID microscopy applications in unshielded environments.

REFERENCES

- [1] A. I. Braginski, *SQUID Sensors: Fundamentals, Fabrication and Applications*, H. Weinstock, Ed. Dordrecht: Kluwer Academic, 1996, NATO ASI Series, p. 235.
- [2] P. Chaudhari, J. Mannhart, D. Dimos, D. D. Tsuei, J. Chi, M. M. Oprysko, and M. Scheuermann, *Phys. Rev. Lett.*, vol. 60, p. 1653, 1988.
- [3] D. Koelle, A. H. Miklich, F. Ludwig, E. Dantsker, D. T. Nemeth, and J. Clark, *Appl. Phys. Lett.*, vol. 63, no. 16, 1993.
- [4] P. Selders, A. Castellanos, M. Vaupel, and R. Woerdenweber, *IEEE Trans. Appl. Superconductivity*, vol. 9, pp. 2967–2970, 1999.
- [5] M. Fardmanesh, J. Schubert, R. Akram, M. Bick, M. Banzet, W. Zander, Y. Zhang, and H.-J. Krause, "Noise, junctions characteristics, and magnetic field dependence of bicrystal grain boundary rf-SQUIDS," in *Applied Superconductivity Conference*, Houston, TX, Aug. 2002.
- [6] M. Fardmanesh, J. Schubert, M. Banzet, W. Zander, Y. Zhang, and J. Krause, *Physica C*, vol. 345, pp. 40–44, 2001.
- [7] Y. Zhang, "Evolution of HTS rf-SQUIDS," *IEEE Trans. Appl. Superconductivity*, vol. 11, pp. 1038–1042, 2001.
- [8] Y. Zhang, N. Wolters, X. H. Zeng, J. Schubert, W. Zander, H. Soltner, H. R. Zi, M. Banzet, F. Ruder, and A. I. Braginski, *Appl. Superconductivity*, vol. 6, pp. 385–390, 1998.
- [9] M. Bick, J. Schubert, M. Fardmanesh, G. Panaitov, M. Banzet, W. Zander, Y. Zhang, and H.-J. Krause, *IEEE Trans. Appl. Superconductivity*, vol. 11, pp. 1339–1342, 2001.
- [10] E. Il'ichev, V. Schultze, R. P. J. IJsselsteijn, R. Stolz, V. Zakosarenko, H.-G. Meyer, and M. Siegel, *Physica C*, vol. 330, pp. 155–159, 2000.
- [11] J. Schubert, M. Siegert, M. Fardmanesh, W. Zander, M. Proempers, C. Buchal, J. Lisoni, and C. H. Lei, *Appl. Surface Science*, vol. 168, pp. 208–214, 2000.
- [12] M. Fardmanesh, J. Schubert, R. Akram, M. Bick, Y. Zhang, M. Banzet, W. Zander, J. Krause, and M. Schilling, *IEEE Trans. Appl. Superconductivity*, vol. 11, pp. 1363–1366, 2001.
- [13] A. Barone and G. Paterno, *Physics and Applications of the Josephson Effect*: Wiley Interscience, 1982.
- [14] E. E. Mitchell, C. P. Foley, K.-H. Mueller, and K. E. Leslie, *Physica C*, vol. 321, pp. 219–230, 1999.
- [15] E. J. Tarte, G. A. Wagner, R. E. Somekh, F. J. Baudenbacher, P. Berghuis, and J. E. Evetts, *IEEE Trans. Appl. Superconductivity*, vol. 7, no. 2, pp. 3662–3665, 1997.
- [16] J.-K. Heinsohn, R. Dittmann, J. R. Contreras, J. Scherbel, A. Klushin, and M. Siegel, *IEEE Trans. Appl. Superconductivity*, vol. 11, no. 1, pp. 795–798, 2001.
- [17] P. A. Rosenthal, M. R. Beasley, K. Char, M. S. Colclough, and G. Zakharchuk, *Appl. Phys. Lett.*, vol. 59, pp. 3482–3484, 1991.